# Study of highly excited vibrational dynamics of HCP integrable system with dynamic potential methods*

Aixing Wang(王爱星)[1,2], Lifeng Sun(孙立风)[3], Chao Fang(房超)[4,†], and Yibao Liu(刘义保)[1]

[1] *Jiangxi Key Laboratory for Mass Spectrometry and Instrumentation, East China University of Technology, Nanchang* 330013, *China*
[2] *School of Science, East China University of Technology, Nanchang* 330013, *China*
[3] *CNNC High Energy Equipment (Tianjin) Co., Ltd, Tianjin* 300300, *China*
[4] *Lab for High Technology, Tsinghua University, Beijing* 100084, *China*

(Received 22 July 2019; revised manuscript received 18 November 2019; accepted manuscript online 20 November 2019)

Highly excited vibrational dynamics of phosphaethyne (HCP) integrable system are investigated based on its dynamic potentials. Taking into consideration the 2:1 Fermi resonance between H–C–P bending vibrational mode and C–P stretching vibrational mode, it is found that the effects of H–C stretching vibrational mode on vibrational dynamic features of the HCP integrable system are significant and regularly vary with Polyad numbers ($P$ number). The geometrical profiles of the dynamic potentials and the corresponding fixed points are sensitive to the variation of H–C stretching vibrational strength when $P$ numbers are small, but are not sensitive when $P$ numbers become larger and the corresponding threshold values become lower. The phase space trajectories of different energy levels in a designated dynamic potential ($P = 28$) were studied and the results indicated that the dynamic potentials govern the various dynamic environments in which the vibrational states lie. Furthermore, action integrals of the energy levels contained in dynamic potential ($P = 28$) were quantitatively analyzed and elucidated. It was determined that the dynamic environments could be identified by the numerical values of the action integrals of trajectories of phase space, which is equivalent with dynamic potentials.

**Keywords:** phosphaethyne (HCP), highly excited vibrational state, fixed point, phase space trajectory

**PACS:** 31.15.–p, 31.50.Df, 05.10.Ln **DOI:** 10.1088/1674-1056/ab593a

## 1. Introduction

Phosphaethyne (HCP) is an essential component of biological molecules and is of great significance in biochemical science.[1] The internal rotation of H atom around the C–P bond in HCP, based on the H–C–P bending vibrational mode, has been of much interest spectroscopically and theoretically since it involves the very basic mechanism in chemical reactions.[2] Studies on the highly excited vibrational dynamics of HCP, especially on its localized bending vibrational characteristics, have been researched thoroughly in previous works.[3,4] The first principles results show that the localized vibration is related to the co-action of Fermi resonances and nonlinear H–C–P bending/C–P stretching vibrational mode in HCP.[5–7] Preliminary quantitative studies on the dynamic potentials of HCP also explain the evolution characteristics of highly excited vibrational dynamics, in the case of large-scale Polyad numbers, and elucidate the dynamic similarities between HCP and deuterated phosphaethyne (DCP) systems.[8]

However, previous studies[1–8] predominantly focused on the Fermi resonance between H–C–P bending mode and C–P stretching mode and neglected to consider the influences of uncoupled H–C vibrational mode of the highly excited vibrational dynamics on the HCP integrable system. Literature reports that the uncoupled mode in triatomic integrable systems significantly affects the dynamic potentials of highly excited vibrational states[9,10] in the DCP system but it is unreasonable to subjective assuming that this conclusion is also correct in the HCP system. On the other hand, the situations and related conclusions of HCP are important for the comparative study of HCP and DCP. In order to solve the above-mentioned questions, this work investigates the highly excited vibrational dynamics of HCP integrable systems by calculating its dynamic potentials. The effects caused by H–C stretching vibrational mode on dynamic features and the phase space trajectories of different energy levels in designated dynamic potentials are studied. Furthermore, action integrals of the energy levels contained in dynamic potentials are calculated and the quantitative analyses are given.

## 2. Semi-classical Hamiltonian of the HCP integrable system

The highly excited energy region of HCP investigated is $6 \times 10^3$ cm$^{-1}$–$1.9 \times 10^4$ cm$^{-1}$ because this range contains numerous dynamic information.[6,7] This energy region has been

*Project supported by the National Natural Science Foundation of China (Grant Nos. 11505027 and 11104156), the Open Foundation of Jiangxi Key Laboratory for Mass Spectrometry and Instrumentation (Grant No. JXMS201605), the Science and Technology Project of Education Department of Jiangxi Province in 2016, and the National High Technology Research and Development Program of China (Grant No. 2014AA052701).

†Corresponding author. E-mail: fangchao@tsinghua.edu.cn

 

studied in our previous work on HCP[8] and the results obtained from this work can be used for comparative analysis. According to the experimental data and simulation results on the second quantization theory representation, the vibrational Hamiltonian is obtained and its corresponding quality coefficients are as follows:[11]

$$\begin{aligned}
&H(n_1,n_2,n_3)\\
&=\omega_1\left(n_1+\frac{1}{2}\right)+\omega_2\left(n_2+\frac{1}{2}\right)+\omega_3\left(n_3+\frac{1}{2}\right)\\
&+X_{11}\left(n_1+\frac{1}{2}\right)^2+X_{12}\left(n_1+\frac{1}{2}\right)(n_2+1)\\
&+X_{13}\left(n_1+\frac{1}{2}\right)\left(n_3+\frac{1}{2}\right)+X_{22}(n_2+1)^2\\
&+X_{23}(n_2+1)\left(n_3+\frac{1}{2}\right)+X_{33}\left(n_3+\frac{1}{2}\right)^2\\
&+y_{222}(n_2+1)^3+z_{2222}(n_2+1)^4\\
&-\left[k+k_1\left(n_1+\frac{1}{2}\right)+k_2(n_2+2)+k_3n_3\right]\\
&\times(a_2^{+2}a_3+a_2^2a_3^+). \qquad (1)
\end{aligned}$$

The subscripts 1, 2, and 3 (denoted by $i$ hereinafter) correspond to H–C stretching vibrational mode, H–C–P bending vibrational mode, and C–P stretching vibrational mode, respectively. $n$ is the quantum number of vibrational modes ($n_i$ denotes the corresponding vibrational mode, whose position coordinate is marked by $q_i$ and momentum coordinate is marked by $p_i$) and $a^+/a$ indicates an increase or decrease of quantum number of the different vibrational modes. $\omega_i$ is the coefficient of simple harmonic oscillation while $X_{ij}$, $y_{ijk}$, and $z_{ijk}$ denote the nonlinear coupling coefficients among different modes. $k_1$, $k_2$, $k_3$, and $k$ represent the Fermi resonance strength coefficients.

**Table 1.** Coefficients of HCP vibrational Hamiltonian.

| Parameter | Values/cm$^{-1}$ | Parameter | Values/cm$^{-1}$ |
|---|---|---|---|
| $\omega_1$ | 3343.12250 | $X_{33}$ | −5.86190 |
| $\omega_2$ | 697.77970 | $y_{222}$ | 0.23345 |
| $\omega_3$ | 1301.08380 | $z_{2222}$ | −0.00562 |
| $X_{11}$ | −55.01610 | $k$ | 3.61150 |
| $X_{12}$ | −16.81740 | $k_1$ | 0.80560 |
| $X_{13}$ | −4.33750 | $k_2$ | 0.06727 |
| $X_{22}$ | −5.34770 | $k_3$ | −0.22067 |
| $X_{23}$ | −4.64600 | | |

A matrix representation of Eq. (1) was obtained by the basis states $|n_1|n_2|n_3\rangle$ and the eigenvalues could be derived through diagonalization. The method of fitting level energies was used to determine the Hamiltonian coefficients and the results are shown in Table 1. The strengths of Fermi resonances vary with quantum numbers of the other three vibrational modes and it can be seen that the strengths of Fermi resonances and nonlinear vibrations in the system are comparable. Considering the 2 : 1 Fermi resonance, there is another conserved quantity named Polyad number besides $n_1$, which is represented as $P=n_2+2n_3$ in this system.[12] From previous studies, it is also known that equation (1) is applicable for determining the dynamics of highly excited vibrational states of HCP integrable system in the region of $n_1<4$, $P<32$.[12]

In order to study the dynamics of HCP integrable systems, the semi-classical representations of Hamiltonian in Eq. (1) are necessary.[8–10] In general, Heisenberg correspondence is usually used to transform the second quantization operators to classical quantities, which is equivalent to the SU(2)/U(1) Lie algebraic coset space representations mathematically.[13] With the standard process,[14] the semi-classical transformation of second quantization operators could be accomplished through the substitution $n_2=\left(q_2^2+p_2^2\right)/2$ and $n_3=[P-\left(q_2^2+p_2^2\right)/2]/2$. With the above canonical transformation, the following equations can be obtained with the ($q_3$, $p_3$) coordinate:

$$\begin{aligned}
&H(n_1,q_2,p_2,P)\\
&=\omega_1\left(n_1+\frac{1}{2}\right)+\omega_2\left(\frac{p_2^2+q_2^2}{2}+\frac{1}{2}\right)\\
&+\omega_3\left(\frac{P}{2}-\frac{p_2^2+q_2^2}{4}+\frac{1}{2}\right)\\
&+X_{11}\left(n_1+\frac{1}{2}\right)^2+X_{12}\left(n_1+\frac{1}{2}\right)\left(\frac{p_2^2+q_2^2}{2}+1\right)\\
&+X_{13}\left(n_1+\frac{1}{2}\right)\left(\frac{P}{2}-\frac{p_2^2+q_2^2}{4}+\frac{1}{2}\right)\\
&+X_{22}\left(\frac{p_2^2+q_2^2}{2}+1\right)^2+X_{23}\left(\frac{p_2^2+q_2^2}{2}+1\right)\\
&\times\left(\frac{P}{2}-\frac{p_2^2+q_2^2}{4}+\frac{1}{2}\right)+X_{33}\left(\frac{P}{2}-\frac{p_2^2+q_2^2}{4}+\frac{1}{2}\right)^2\\
&+y_{222}\left(\frac{p_2^2+q_2^2}{2}+1\right)^3+z_{2222}\left(\frac{p_2^2+q_2^2}{2}+\frac{1}{2}\right)^4\\
&-\left[k+k_1(n_1+\frac{1}{2})+k_2\left(\frac{p_2^2+q_2^2}{2}+2\right)\right.\\
&\left.+k_3\left(\frac{P}{2}-\frac{p_2^2+q_2^2}{4}\right)\right]\sqrt{\frac{P}{2}-\frac{p_2^2+q_2^2}{4}}(q_2^2-p_2^2), \qquad (2)
\end{aligned}$$

the Hamiltonian can also be written with the substitution $n_3=\left(q_3^2+p_3^2\right)/2$ and $n_2=P-\left(q_3^2+p_3^2\right)$ as follows:

$$\begin{aligned}
&H(n_1,q_3,p_3,P)\\
&=\omega_1\left(n_1+\frac{1}{2}\right)+\omega_2(P-p_3^2-q_3^2+1)\\
&+\omega_3\left(\frac{p_3^2+q_3^2}{2}+\frac{1}{2}\right)+X_{11}\left(n_1+\frac{1}{2}\right)^2+X_{12}\left(n_1+\frac{1}{2}\right)\\
&\times(P-p_3^2-q_3^2+1)+X_{13}\left(n_1+\frac{1}{2}\right)\left(\frac{p_3^2+q_3^2}{2}+\frac{1}{2}\right)
\end{aligned}$$

$$+X_{22}(P-p_3^2-q_3^2+1)^2+X_{23}(P-p_3^2-q_3^2+1)$$
$$\times\left(\frac{p_3^2+q_3^2}{2}+\frac{1}{2}\right)+X_{33}\left(\frac{p_3^2+q_3^2}{2}+\frac{1}{2}\right)^2$$
$$+y_{222}(P-p_3^2-q_3^2+1)^3+z_{2222}(P-p_3^2-q_3^2+1)^4$$
$$-\left[k+k_1\left(n_1+\frac{1}{2}\right)+k_2(P-p_3^2-q_3^2+2)\right.$$
$$\left.+k_3\left(\frac{p_3^2+q_3^2}{2}\right)\right]\sqrt{2}(P-p_3^2-q_3^2)q_3. \quad (3)$$

## 3. Analysis of highly excited vibrational states of HCP integrable system with dynamic potentials approach

The semi-classical Hamiltonian obtained in Eqs. (2) and (3) can be used in solving the dynamic potentials corresponding $P$ numbers of the highly excited vibrational states of HCP integrable system. The dynamic potential of $H(q_i,p_i)$ is the effective environment in which the $q_i$ coordinate experiences, and it can be achieved by calculating the maximal and minimal energies by varying $p_i$ for each $q_i$ under the boundary conditions where actions ($n_i$) are non-negative. Geometrically speaking, the dynamic potential composed of these maximal and minimal energies as a function of $q_i$ is a closed curve in which the quantized levels are enclosed. The $q_i$ region for each level in which the dynamic potential encloses is also defined and observed. Dynamic potential supplies a channel of studying the dynamic feature of highly excited vibrational states with intuitional physical pictures instead of complicated calculations. In the past ten years, the framework and applications of dynamic potential have been developed very well and sufficient results have been achieved in the studying of highly excited vibrational states of integrable and non-integrable molecular systems.[8–10] For $H(q_2,p_2)$, the boundary condition can be expressed as $q_2^2+p_2^2<2P$, which is obtained from $n_2=\left(q_2^2+p_2^2\right)/2>0$ and $n_3=[P-\left(q_2^2+p_2^2\right)/2]/2>0$. For $H(q_3,p_3)$, the boundary condition can also be expressed as $q_3^2+p_3^2<P$ which is obtained from $n_3=\left(q_3^2+p_3^2\right)/2>0$ and $n_2=[P-2\times\left(q_3^2+p_3^2\right)/2]>0$. The dynamic potential composed of these maximal and minimal energies as a function of $q_i$ is a closed curve.[15] The points in the dynamic potential corresponding to $\partial H/\partial q_i=0$ are named as "fixed points" of motion trajectories in the dynamic space, and represent the stable or unstable states of vibration.

In the following sections, two key parts are addressed: (i) the influence of H–C stretching vibrational mode on the dynamic features of HCP governed by small, medium, and large $P$ numbers ($P=12$, 22, and 28 respectively); (ii) the phase space trajectories for each of the energy levels in the dynamic potentials, when $P=30$ as a case study.

### 3.1. Dynamic potentials and their features with different quantum numbers $n_1$ governed by typical Polyad numbers

The dynamic potentials, represented by coordinates $q_2$ and $q_3$ of the HCP system, with different $P$ numbers when $n_i=0\sim3$ are shown in the following figures (Figs. 1–3). The fixed points of bending vibration are denoted as [B] and the fixed points of C–P stretching vibration are denoted as [R]. Superscript $*$ is for the secondary appearance of [R] or [B] and the bar on top of [R] or [B] represents an unstable fixed point. The subscript "2" or "3" shows the coordinates ($q_2$ or $q_3$) at which the fixed point appears.

The results of the small $P$ number ($P=12$) are given in Fig. 1, and it shows that the profiles of dynamic potentials ($q_2$ and $q_3$) vary when they coordinate with different $n_1$. The profiles of dynamic potentials represented with $q_2$ vary significantly from $n_1=0$ to 2 gradually but remain almost the same from $n_1=2$ to 3. This indicates that the effects of H–C stretching vibrational mode on H–C–P bending vibrational mode are not observable when the strength of $n_1$ mode reaches a threshold. The dynamic potentials represented with $q_2$ coordinates, had localized modes[12] appear gradually at the bottom of the dynamic potentials with the strengthening of the H–C stretching vibration (increase of the value of $n_1$). By contrast, the profiles of dynamic potential represented by $q_3$ when $n_1=0$ are different in cases when $n_1\neq0$. Furthermore, the concave invariance remained when $n_1=1$, 2, 3, which demonstrates the influence of H–C stretching vibrational mode to H–C–P bending vibrational mode and C–P vibrational mode, is different. On the other hand, it is well known that the fixed points shown in the dynamic potentials are easily identified to govern various dynamic environments in which the vibrational states lie.[9,10,15] In Fig. 1, it is accessible to find that the numbers of fixed points in the dynamic potentials represented by $q_2$ decrease gradually. When the value of $n_1$ is increased, it is elucidated that though H–C stretching vibrational mode is not considered as a coupled mode, it still affects the dynamic features of the HCP integrable system. For this reason, the reconsideration of uncoupled H–C stretching vibrational mode in the Hamiltonian of the HCP integrable system makes sense.

The results of medium $P$ number ($P=22$) are shown in Fig. 2. For the dynamic potentials represented by $q_2$, some fixed points ([B2] and [$\overline{\text{B2}}$ ]) disappear with an increase in the value of quantum number $n_1$, indicating that the dynamic potential pattern of H–C–P bending vibrational mode tends to be simpler, rather than more complicated with the strengthening of H–C stretching vibration. This variation also indicates that the action of H–C stretching vibrational mode weakened the

coupling 2 : 1 Fermi resonance between H–C–P bending vibrational mode and C–P stretching vibrational mode, which is different from the results of DCP integrable system.[16] Compared with the case of $P = 12$, it is found that when $n_1 = 1$, 2, 3, the profiles of dynamic potentials represented with $q_2$ are almost the same but are significantly different from $n_1 = 0$. This shows that the influence of H–C stretching vibrational mode is weakening the $P$ number increases and the threshold ($n_1$ value) becomes low. This phenomenon was first observed in the study of dynamic potentials of highly excited vibrational states in triatomic molecular integrable system, and is different when compared with the results of HOCl, HOBr, and DCP integrable systems.[9,10,16] For the dynamic potentials represented with $q_3$, the concave invariance remained when $n_1 = 0$–3 and the number of energy levels contained within the inverse Morse potential[8–10] reduced whereas the Morse potential increased. Based on the above-mentioned results, it is clear that the influence of H–C stretching vibrational mode to C–P stretching vibrational mode is moderate and is very prominent in the H–C–P bending vibrational mode.

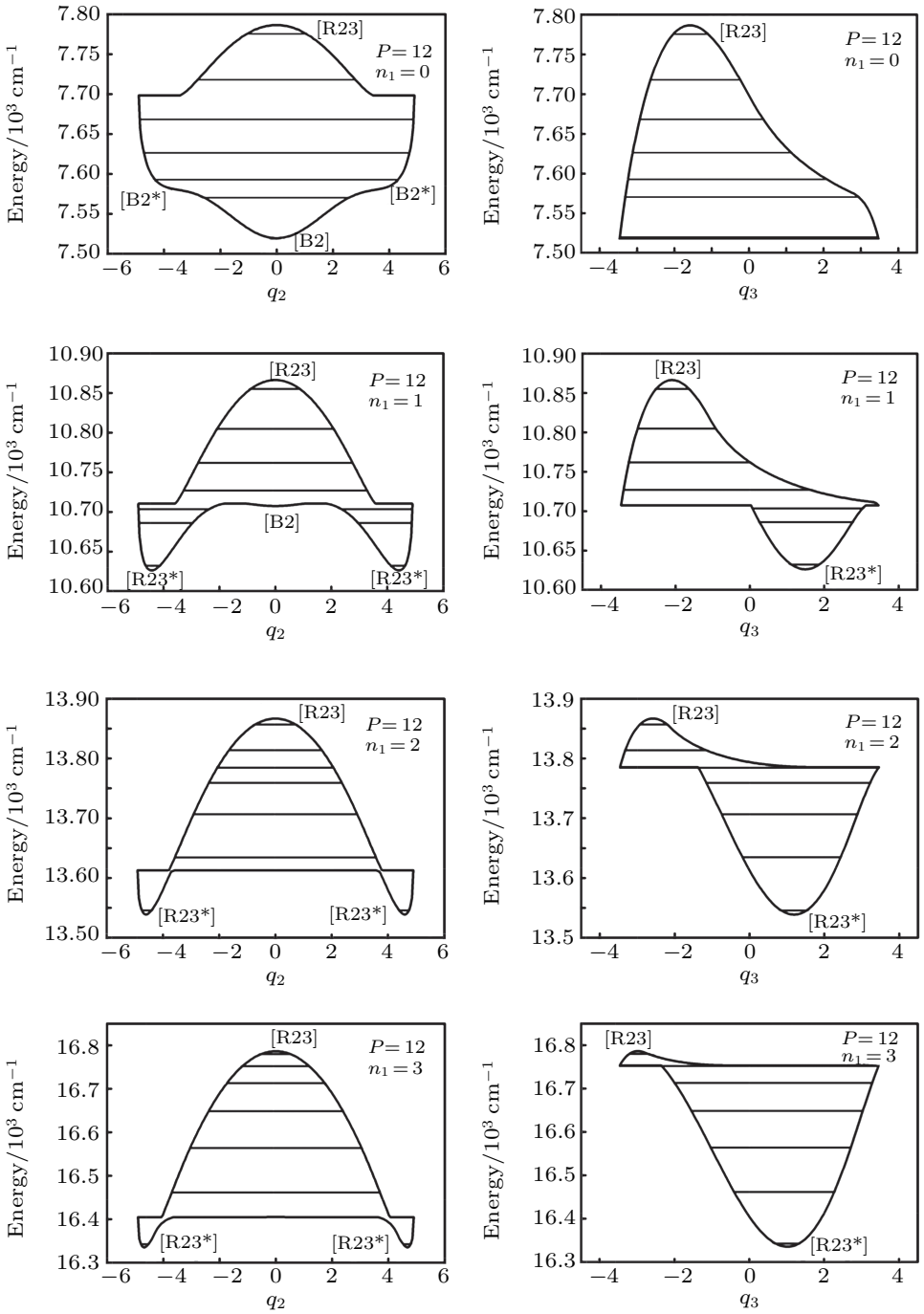


**Fig. 1.** Dynamic potentials of HCP ($P = 12$) with $n_1 = 0 \sim 3$ (the energy levels within potentials are marked by horizontal lines).

The deformations of dynamic potentials and corresponding features of the H–C–P integrable systems are much simpler when the $P$ number is large. For instance, the dynamic potentials when $P = 28$ are shown in Fig. 3. The patterns of dynamic potentials represented with $q_2$ when $n_1 = 0 \sim 3$ are similar and very monotonous. The phenomenon is also similar in dynamic potentials represented with $q_3$, except that the numbers of energy levels within the inverse Morse potential and Morse potential vary widely, which can also be observed for the case of $P = 12$ and $P = 22$. From a topological perspective, there is concave invariance in dynamic potentials represented with $q_2$ and $q_3$, respectively when the $P$ number is large and verifies again so that the influence of H–C stretching vibrational mode is weakened with an increase in $P$ number. Quantitatively, the threshold of $n_1$ disappears when the $P$ number is large.

Based on these studies, it shows that the H–C stretching mode affects the resonant coupling of H–C–P bending and C–P stretching modes on some levels, thereby affecting the dynamic features of the HCP integrable system. The geometrical profiles of the dynamic potentials and the corresponding fixed points are sensitive to the variation of H–C stretching vibrational mode when the $P$ number is small, but are not sensitive when the $P$ number is large and the corresponding threshold value ($n_1$) is becoming low. Though the cases of $P = 12$, 22, and 28 are shown here, these conclusions are universal for HCP integrable systems and the dynamic potentials due to their typical topological structures and corresponding abundant connotations.

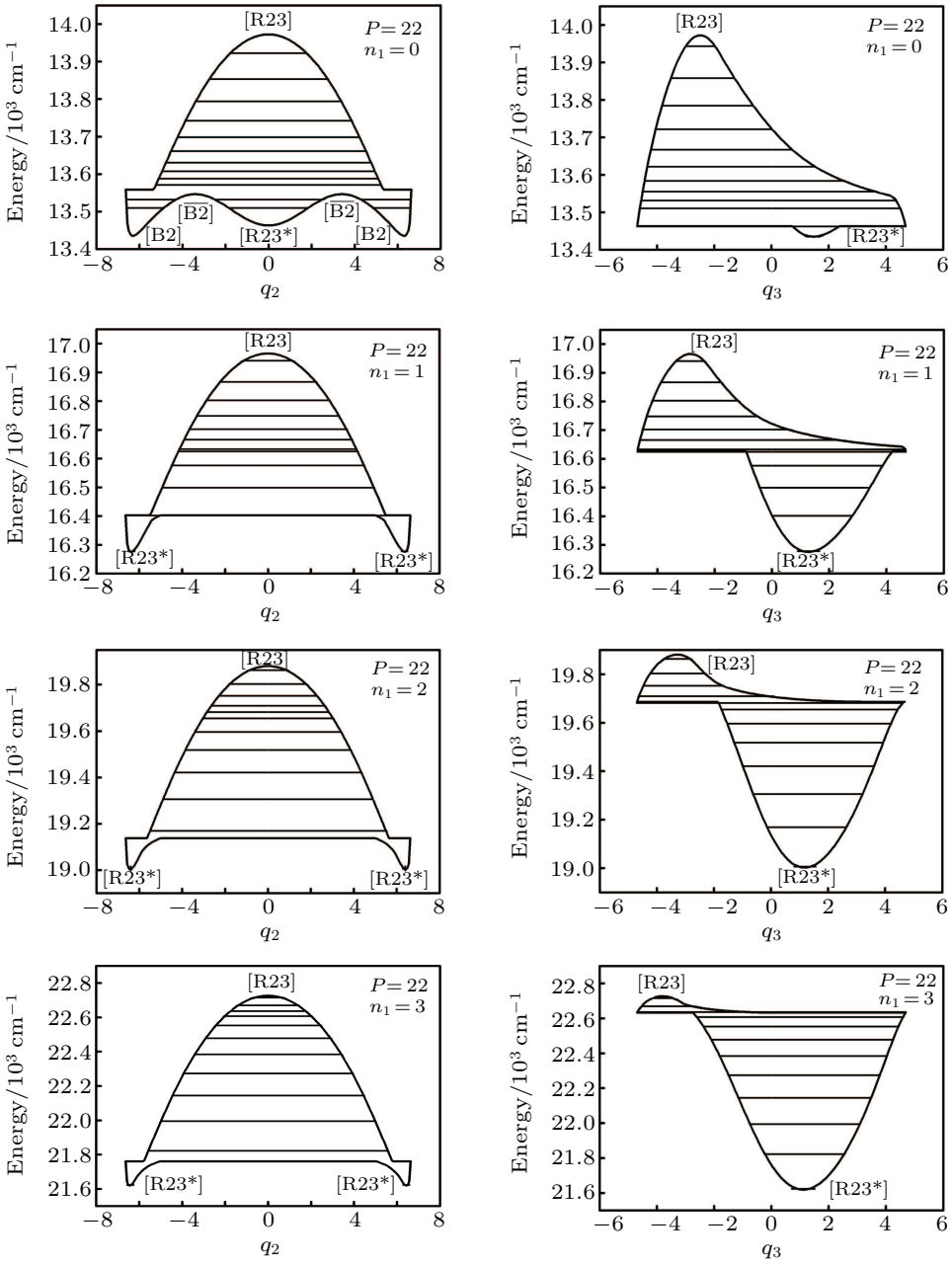


**Fig. 2.** Dynamic potentials of HCP ($P = 22$) with $n_1 = 0 \sim 3$ (the energy levels within potentials are marked by horizontal lines).

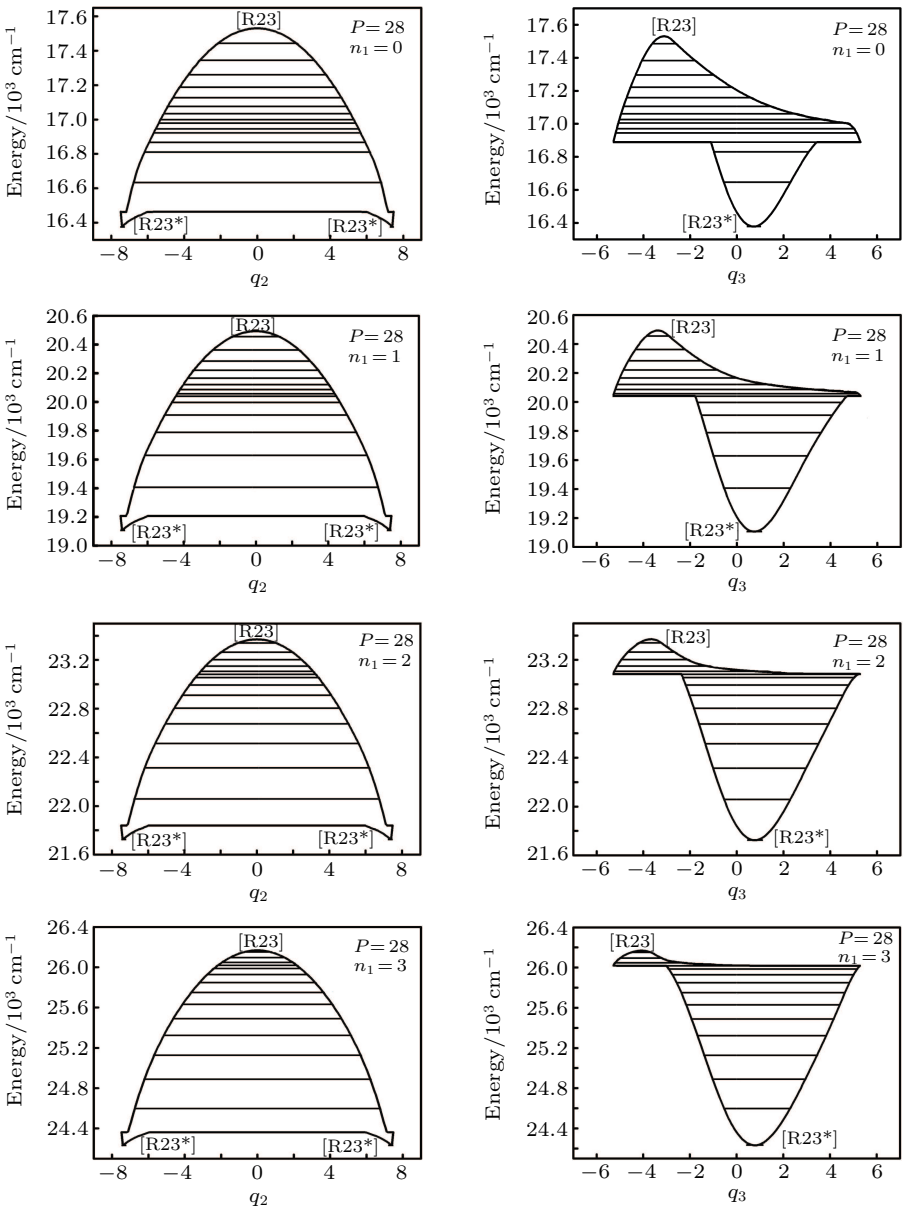


**Fig. 3.** Dynamic potentials of HCP ($P = 28$) when $n_1 = 0 \sim 3$ (the energy levels within potentials are marked by horizontal lines).

### 3.2. Trajectories of phase space and dynamic environment of energy levels with specific Polyad number ($P = 28$)

The properties of the dynamic potentials were analyzed qualitatively with different quantum numbers $n_1$ and Polyad numbers. An in-depth analysis of the characteristic for all energy levels in the HCP integrable system was conducted through its $p_i$–$q_i$ phase diagram. The dynamic potentials represented with $q_2$ and $q_3$ when $P = 28$ and $n_1 = 0$ is shown in Fig. 4, where the horizontal lines show the energy levels sharing the designated $P$ number. The variables $P = 28$ and $n_1 = 0$ were chosen in this study due to their representative and successful characteristics. All conclusions shown in the following section is universal for any designated $P$ and $n_1 = 0$, only if the corresponding Hamiltonian is suitable for the HCP integrable system.

Figure 4 illustrates that the upper part of dynamic potentials (the region of high energy) is seen as an inverse Morse potential while the bottom of dynamic potentials (the region of low energy) is revealed as a Morse potential. This resulted for both coordinates $q_2$ and $q_3$, indicating that the dynamic environment of the highly excited vibrational states corresponding to high and low energy levels are different. It is well known that the vibrational characteristics of every energy level in the dynamic potential could be described visually by drawing $p_i$–$q_i$ trajectories in phase space.[17,18] Through geometric analyzing the trajectories of L0–L14, it is advisable to divide the 15 $p_i$–$q_i$ trajectories into several classes. It is found that all 15 into $p_2$–$q_2$ trajectories corresponding to 15 energy levels of the dynamic potential, represented with $q_2$, can be divided into five classes: L0–L7, L8, L9–L10, L11–L13, L14. It is

comparable to divide all 15 $p_3$–$q_3$ trajectories of the dynamic potential, represented with $q_3$, into four classes: L0–L8, L9–L10, L11–L13, L14. The representative trajectories $p_2$–$q_2$ and $p_3$–$q_3$ are shown in Fig. 5 and Fig. 6.

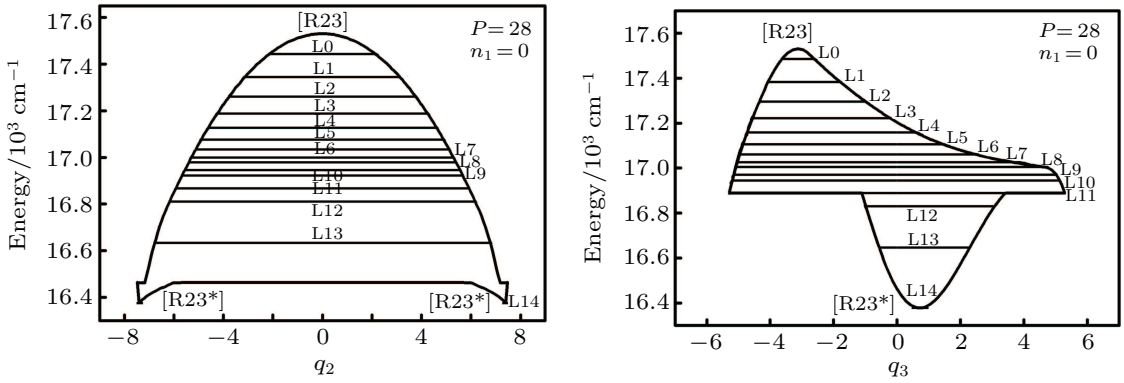


**Fig. 4.** Dynamic potentials of HCP when $P = 28$ and $n_1 = 0$. L0–L14 represent the energy levels included in the dynamic system.

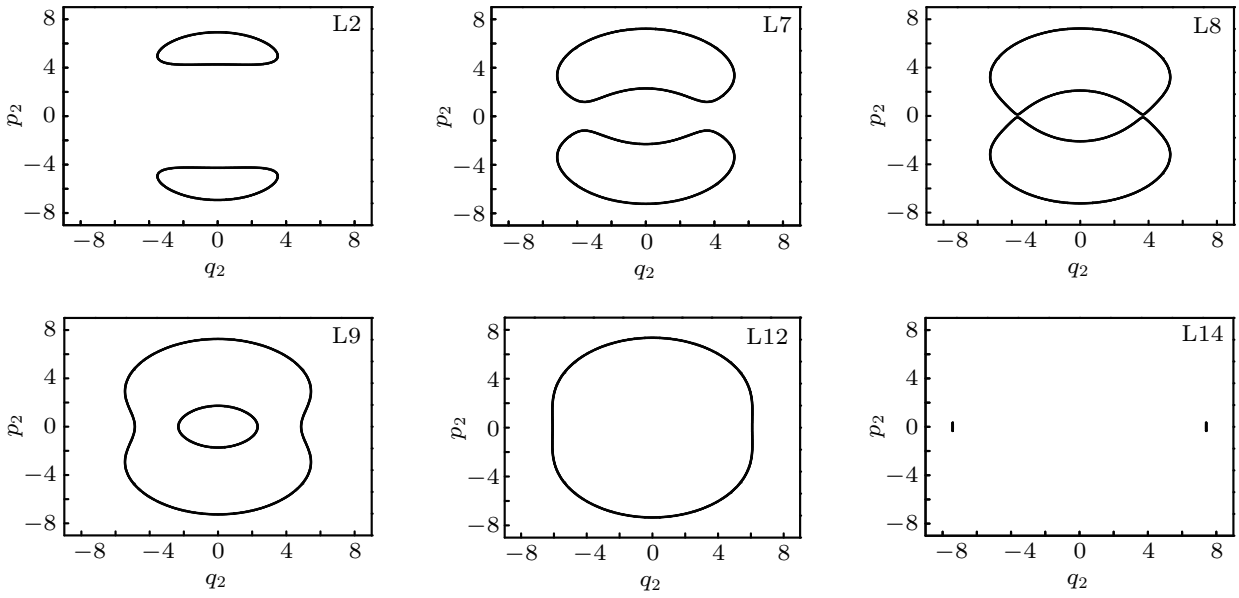


**Fig. 5.** Trajectories of phase space of L2, L7, L8, L9, L12, L14 when $P = 28$ and $n_1 = 0$ ($q_2$ coordinates).

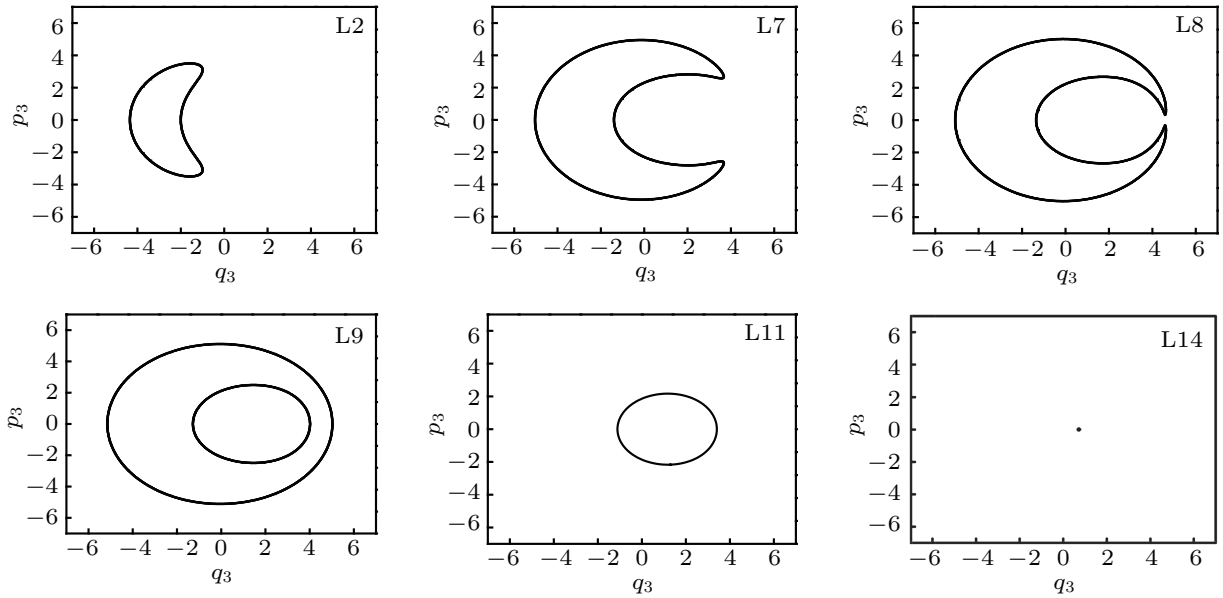


**Fig. 6.** Trajectories of phase space of L2, L7, L8, L9, L11, L14 when $P = 28$ and $n_1 = 0$ ($q_3$ coordinates).

Both in Figs. 5 and 6, continuous variations of phase trajectories are observed visually. In Fig. 5, energy levels L0–L13 are in the region of the inverse Morse potential and the corresponding areas of phase trajectories are increasing with the descend of energy values. L14 is at the bottom of the Morse potential and its corresponding area of phase trajectory is the minimum value. The localized bending vibrational mode is revealed in the phase trajectory as separated $q$-space pattern. In Fig. 6, it is shown that the energy levels L0–L10 are in the inverse Morse potential and the corresponding areas of phase trajectories are increasing with the descend of energy values. L11–L14 are found within the Morse potential and their corresponding areas of phase diagrams decrease with decreasing energy values. From the above results, it is elucidated that the dynamic potentials govern the various dynamic environments in which the vibrational states lie.

Furthermore, based on the quantitative study of the dynamic environments of each energy level, the action integrals of the phase space trajectories are calculated with the following formula:[8]

$$\text{Action integral} = \frac{1}{2\pi} \times \oint p_i \mathrm{d}q_i, \tag{4}$$

the results are shown in Table 2.

**Table 2.** Action integrals of energy levels corresponding to $P = 28$, $n_1 = 0$.

| State label | Action integral in ($q_2$, $p_2$) space | Difference of action integrals of neighboring states | State label | Action integral in ($q_3$, $p_3$) space | Difference of action integrals of neighboring states |
|---|---|---|---|---|---|
| L0 | 0.8278 | – | L0 | 0.3920 | – |
| L1 | 2.8002 | 1.9724 | L1 | 1.4007 | 1.0087 |
| L2 | 4.8166 | 2.0164 | L2 | 2.4090 | 1.0083 |
| L3 | 6.8315 | 2.0149 | L3 | 3.4166 | 1.0076 |
| L4 | 8.8454 | 2.0139 | L4 | 4.4236 | 1.007 |
| L5 | 10.8595 | 2.0141 | L5 | 5.4304 | 1.0068 |
| L6 | 12.8702 | 2.0107 | L6 | 6.4354 | 1.005 |
| L7 | 14.9470 | 2.0768 | L7 | 7.4733 | 1.0379 |
| L8 | 16.6763 | 1.7293 | L8 | 8.3352 | 0.8619 |
| L9 | 19.3764 | 2.7001 | L9 | 9.6876 | 1.3524 |
| L10 | 20.6888 | 1.3124 | L10 | 10.3439 | 0.6563 |
| L11 | 23.0884 | 2.3996 | L11 | 2.4534 | – |
| L12 | 23.9827 | 0.8943 | L12 | 2.0060 | 0.4474 |
| L13 | 25.9835 | 2.0008 | L13 | 1.0028 | 1.0032 |
| L14 | 0.0006 | – | L14 | 0.0017 | 1.0011 |

Table 2 shows the action integrals for the energy levels when $P = 28$, which are calculated based on the trajectory areas of the phase space represented with ($q_2$, $p_2$) and ($q_3$, $p_3$). From the action integrals of trajectories ($q_2$, $p_2$), it is found that the action integrals increase in a constant step with the decrease in the corresponding energy levels since they lie in the inverse Morse potentials (L14 is not considered here because it is an independent localized mode). From the action integrals calculated from ($q_3$, $p_3$) space, they are grouped into two subsets: L0 to L10 and L11 to L14. For the former ones, the action integrals increase with the decrease in the corresponding energy levels due to the inverse Morse potentials where they are located. For the latter ones, the action integrals decrease with the decrease in the corresponding energy levels due to the Morse potentials where they are located.

The constant action integral increment/decrement demonstrates the compatibility of our classical treatment with the quantized levels. It also shows that the levels stay in various dynamic environments, which are defined essentially by the dynamic potential with a designated Polyad number. In addition, from the action integrals obtained from ($q_2$, $p_2$) space, the differences between adjacent energy levels' action integrals are almost always the same (it approximately equals 1, but the L10 and L12 are exceptions and should be further studied in the future). The corresponding results obtained from ($q_3$, $p_3$) space are equal to 2, which correspond to the 2 : 1 Fermi resonance in the HCP integrable system. It is also demonstrated that the dynamic potentials are equivalent to the trajectories in space phase and can depict the dynamic environments in which individual energy levels are located.[19]

## 4. Conclusions and remarks

The analysis of HCP revealed that H–C stretching vibrational mode ($n_1$) has impacts on the dynamic potentials of vibrational mode with the $P$ number as a deciding factor to such impacts. In detail, H–C stretching vibrational mode has a strong impact on the profiles of the dynamic potentials, represented with $q_2$ and $q_3$, when the $P$ number is small and the threshold ($n_1$ value) is observed. However, the influence of H–C stretching vibrational mode is becoming weak and even negligible as the $P$ number increases. These results indicate that the H–C stretching vibrational mode affects the dynamics

of both the H–C–P bending vibrational mode and C–P stretching vibrational mode, when there is a 2 : 1 Fermi resonance in the HCP integrable system. In other words, it is elucidated that the 2 : 1 Fermi resonance model of HCP integrable systems is feasible when the $P$ number is large enough. When the $P$ number is small, the H–C stretching vibrational mode should be considered as another coupled mode. Additionally, the differences between adjacent energy level action integrals in $(q_2, p_2)$ space are twice those of the ones in $(q_3, p_3)$ space, which are congruent with the 2 : 1 Fermi resonance in HCP integrable systems. It is determined that the dynamic environments can be identified by the numerical values of action integrals, which are equivalent to dynamic potentials.

## References


[1] Gier T E 1961 *J. Am. Chem. Soc.* **83** 1769

[2] Joyeux M, Sugny D, Tyng V, Kellman M, Ishikawa H, Field R W, Beck C and Schinke R 2000 *J. Chem. Phys.* **112** 4162

[3] Farantos S C, Keller H, Schinke R, Yamashita K and Morokuma K 1996 *J. Chem. Phys.* **104** 10055

[4] Ishikawa H, Field R W, Farantos S C, Joyeux M, Koput J, Beck C and Schinke R 1999 *Ann. Rev. Phys. Chem.* **50** 443

[5] Ishikawa H, Nagao C, Mikami N and Field R W 1997 *J. Chem. Phys.* **106** 2980

[6] Ishikawa H, Chen Y T, Ohshima Y, Wang J and Field R W 1996 *J. Chem. Phys.* **105** 7383

[7] Ishikawa H, Nagao C, Mikami N and Field R W 1998 *J. Chem. Phys.* **109** 492

[8] Fang C and Wu G 2009 *J. Mol. Struc. Theochem* **910** 141

[9] Wang A X, Liu Y B and Fang C 2012 *Acta. Phys. Sin.* **61** 053102 (in Chinese)

[10] Wang A X, Sun L F, Fang C and Liu Y B 2013 *Int. J. Mol. Sci.* **14** 5250

[11] Beck C, Schinke R and Koput J 2000 *J. Chem. Phys.* **112** 8446

[12] Joyeux M, Grebenshchikov S Y and Schinke R 1998 *J. Chem. Phys.* **109** 8342

[13] Zhang W M, Feng D H and Gilmore R 1990 *Rev. Mod. Phys.* **62** 867

[14] Joyeux M, Sugny D, Lombardi M, Jost R, Schinke R, Skokov S and Bowman J 2000 *J. Chem. Phys.* **113** 9610

[15] Fang C and Wu G Z 2009 *Chin. Phys. B* **18** 130

[16] Wang A X, Fang C and Liu Y B 2016 *Int. J. Mol. Sci.* **17** 1280

[17] Zhang C, Fang C and Wu G Z 2010 *Chin. Phys. B* **19** 110513

[18] Fang C and Wu G Z 2010 *Chin. Phys. B* **19** 010509

[19] Wang A X, Fang C and Liu Y B 2017 *Molecules* **22** 101